# HVEM blockade initiates tumor cell death by innate immunity and improves anti-tumor response by human T cells in NSG immuno-compromised mice

Brunel S.[1*], Aubert N. [1*], KC P. [1], Olive D.[2] and Marodon G.[1≠]

1 Sorbonne Universités, Inserm, CNRS, Centre d'immunologie et maladies infectieuses-Paris, Cimi-Paris, Paris 75013, France

2 Institut Paoli-Calmettes, Aix-Marseille Université, Inserm, CNRS, CRCM, Tumor Immunity Team, IBISA Immunomonitoring platform, Marseille, France

* Equal contributions

≠ Corresponding author: gilles.marodon@inserm.fr, Sorbonne Universités, Inserm, CNRS, Centre d'immunologie et maladies infectieuses-Paris, Cimi-Paris, Paris 75013, France

Keywords: HVEM; monoclonal antibody; cancer immunotherapy; humanized mice

Abbreviations: HVEM, Herpes Virus Entry Mediator; BTLA, B and T Lymphocyte Attenuator; TNFRSF, Tumor Necrosis Factor Receptor Superfamily; NSG, NOD.SCID.$\gamma c^{null}$ ; monoclonal antibody, mAb; ADCP, Antibody Dependent Cellular Phagocytosis; ICI, Immune Checkpoint Inhibitors

**Abstract**

Members of the TNF receptor superfamily (TNFRSF) are attractive targets for cancer immunotherapy. Here, we investigated the impact on tumor growth of a murine monoclonal antibody to human TNFRSF14 (HVEM) in PBMC-humanized NSG mice. We first showed that injection of the anti-HVEM monoclonal antibody led to a reduction in the growth of a human HVEM-expressing prostate cancer cell line, associated to an increase in the proliferation and number of TIL. These results were not reproduced if the tumor was engineered not to express HVEM by CRISPR/Cas9. We observed a similar effect of the antibody on tumor growth in non-humanized NSG mice that was also lost with the HVEM-deficient cell line. These results suggest that the antibody exerted its anti-tumor effect by directly binding to tumor cells. However, *in vitro* microscopy analysis showed that the antibody alone had no significant effect on tumor survival. In contrast, addition of peritoneal macrophages from NSG mice to the culture resulted in tumor killing and slower growth of the tumor, suggesting that innate immunity of NSG mice participated in tumor control *in vivo*. Finally, we reproduced the *in vivo* anti-tumor effect of the antibody on a human melanoma $HVEM^+$ cell line, suggesting that the therapy could be applied to various $HVEM^+$ cancers. Altogether, our results suggest that therapeutic efficacy of the antibody is associated to cell death mediated by innate immune cells, allowing subsequent human T cell-mediated immunity to control tumor growth.

## Introduction

Immune escape by tumor is now considered a hallmark of cancer (1). Many immune mechanisms are involved to explain loss of tumor control, including defective MHC function and expression, recruitment of suppressive immune cells or expression of co-inhibitory receptors such as PD-L1 (2). In the last few years, targeting co-inhibitory molecules (that can be expressed by tumor or immune cells) with antibodies showed impressive results in tumor regression and overall survival, leading to approval of anti-CTLA-4, anti-PD1 and anti-PD-L1 in numerous cancers (3). However, the success of immune checkpoint inhibitors (ICI) is still partial and many patients fail to respond. Limited tumor infiltrate (cold tumors) or low expression of the targeted molecule may explain the relative inefficiency of ICI (4,5). To overcome these limitations, it is necessary to explore other pathways that might be involved in immune escape and that could complement actual therapies.

Recently, a new co-inhibitory pair has been highlighted in anti-tumor immune response: HVEM (Herpes Virus Entry Mediator, TNFRSF14) and BTLA (B and T lymphocyte attenuator). These two molecules can be expressed by many immune cells including T-cells, in which signaling through BTLA is associated to inhibition of their activation (6,7). Additionally, the HVEM network includes many additional partners, such as LIGHT, lymphotoxin α (LTα) or CD160 (8). Like BTLA, binding of HVEM to CD160 on T-cells is associated with an inhibition of their activation (9). On the other side, stimulation of HVEM on T-cells by any of its ligands is associated with proliferation, survival and inflammatory cytokines production, such as IL-2 and IFN-γ (9,10). Several clinical studies have shown that HVEM expression is upregulated in many types of cancers including colorectal cancers (11), esophageal carcinomas (12), gastric cancers (13), hepatocarcinomas (14), breast cancers (15) or lymphomas (16). In these studies, high level of HVEM expression by tumors were associated with worse prognosis and lower survival. Moreover, HVEM expression by tumors was also associated with a reduction of CD4 and CD8 tumor-infiltrating lymphocytes (TIL) numbers (11,12,14).

Few studies considered affecting tumor growth by targeting the HVEM network. In fact, strategies to inhibit HVEM expression by tumors, by competing for its ligands or directly stimulating HVEM expressed on T-cells, lead to increased T cell proliferation and function in syngeneic mouse models (12,17–19). However, to our knowledge, no study so far has assessed the possibility to use a monoclonal antibody (mAb) to HVEM to favor the anti-tumor immune response and *a fortiori* in a humanized context *in vivo*.

Herein, we explored the therapeutic potential of a murine antibody targeting human HVEM in a humanized mice model grafted with various human tumor cell lines, which express HVEM or

engineered not to express HVEM by CRISPR/Cas9. To generate humanized mice, we used immuno-compromised NOD.SCID.$\gamma c^{null}$ (NSG) mice which are deprived of murine T-, B- and NK-cells but that retain functionally immature macrophages and multinucleated cells (20). We reconstituted these mice with human PBMC, allowing us to study the effect of our antibody on both tumor, murine myeloid cells and human T-cells. Our results strongly advocate for the clinical implementation of anti-HVEM mAbs for cancer immunotherapy of $HVEM^+$ tumors and provide some clues on the mechanism of action of the mAb *in vivo*.

## Materials & Methods

*Preparation of human peripheral mononuclear cells*

Human peripheral blood mononuclear cells were collected by Etablissement Français du Sang from healthy adult volunteers after informed consent in accordance with the Declaration of Helsinki and isolated on a Ficoll gradient (Biocoll). Cells were washed in PBS 3% FCS and diluted at the appropriate concentration in 1× PBS before injection into mice.

*Humanized mice tumor model*

All animals used were NSG mice (stock ≠005557) purchased from the Jackson laboratory (USA). Mice were bred in our animal facility under specific pathogen-free conditions in accordance with current European legislation. All protocols were approved by the Ethics Committee for Animal Experimentation Charles Darwin (Ce5/2012/025). To assess therapeutic activity, 8–20-weeks-old NSG mice (males and females) were injected subcutaneously with $2.10^6$ tumour cells. One week later, mice were irradiated (2 Gy) and engrafted the same day with $2.10^6$ huPBMC by retro orbital injection. 4-5 days after transplantation, the anti-huHVEM antibody or isotype control was injected intra peritoneally at 2 mg/kg. General state, body weight and survival of mice were monitored every 2 days to evaluate Graft-vs-Host-Disease (GVHD) progression. Mice were euthanised when exhibiting signs of GVHD, such as hunched back, ruffled fur, and reduced mobility.

*Antibodies*

The clone 18.10 has been described previously (21). Briefly, 18.10 is a murine IgG1 anti-human HVEM mAb and was produced as ascites and purified by protein A binding and elution with the Affi-gel Protein A MAPS II Kit (Bio-rad). Mouse IgG1 isotype control (clone MOPC-21), rat IgG2b anti-Gr1 (clone RB6-8C5) and isotype control (clone LTF-2) were purchased from Bio X Cell (West Lebanon, NH, USA).

*Cell lines*

PC3 (non-hormone-dependant human prostate cancer cells), Gerlach (human melanoma cells), MDA-MB-231 (breast cancer cells) were grown in high glucose DMEM media supplemented with 10% FCS, L-glutamine and antibiotics (Penicillin/Streptomycin). PC3 and MDA-MB-231 were genetically authenticated (Eurofins). All cells were confirmed to be free of mycoplasmas before injection into mice by the MycoAlert detection kit (Lonza). Tumor growth was monitored using an electronic calliper and volumes were determined using the following formula: $[(\text{length}*\text{witdh}^2)/2]$

*Generation of HVEM deficient PC3 clone using CRISPR-Cas9 technology*

50,000 PC3 cells were seeded in a 24-well plate. Twenty-four hours later, cells were incubated with sgRNA complementary to exon3 of HVEM (GCCAUUGAGGUGGGCAAUGU + Scaffold, TrueGuide Synthtetic guide RNAs, Invitrogen™), Cas9 nuclease (TrueCut™ Cas9 Protein v2, Invitrogen™) and lipofectamine (Lipofectamine™ CRISPRMAX™ Cas9 Transfection Reagent, Invitrogen™) according to manufacturer instructions (TrueCut Cas9 protein v2). After three days, efficiency was evaluated with GeneArt Genomic Cleavage Detection Kit (Invitrogen™) according to the manufacturer instructions. For this assay, DNA was amplified with the following primers: TGCGAAGTTCCCACTCTCTG (Forward) and GGATAAGGGTCAGTCGCCAA (Reverse). Cells were cloned by limiting dilution in 96-well plates. Clones were screened for HVEM expression by flow cytometry using anti-HVEM (clone 94801, BD) and were considered as negative if HVEM expression was undetectable for at least 3 subsequent measurements over the course of one month.

*In vitro assays*

PC3 cells were seeded in 96-wells plate at 7000 cells/well in RPMI medium. Macrophages from NSG mice were obtained by peritoneal wash. The target to effector ratio was 1:10 for cell death evaluation and 1:5 for apoptosis monitoring. Cells were treated by the anti HVEM antibody or its isotype control MOPC21 at 10µg/ml. Cell death was evaluated by flow cytometry after 16 hours of incubation (37°C, 5%CO2) by 7AAD staining. Apoptosis was assessed and analysed every hour by macroscopic live cell analysis (Incucyte®), with PC3-GFP cell line generated in the laboratory by lentiviral transduction and apoptotic specific reagent (Incucyte annexin V red reagent for apoptosis (#4641) Sartorius) used according to the supplier recommendation.

*Phenotypic analysis by flow cytometry*

Tumors were digested with 0.84mg/mL of collagenase IV and 10µg/mL DNAse I (Sigma Aldrich) for 40min at 37°C with an intermediate flushing of the tissue. Cells were passed through a 100µm-cell strainer and resuspended in PBS 3% SVF. To eliminate dead cells and debris, tumor cell suspensions were isolated on a Ficoll gradient. Rings were collected, washed, and cell pellets were resuspended in PBS 3%SVF before counting on LUNA™ Automated Cell counter (Logos Biosystems). Subsequently, up to $2.10^6$ live cells were stained with viability dye (eF506, Fixable Viability Dye, ThermoFisher) for 12min at 4°C, Fc receptor were blocked with human FcR Blocking Reagent (120-000-442, Miltenyi Biotec) and anti-CD16/32 (clone 2.4G2) for 10min. The followings antibodies were added for 35min

at 4°C: hCD45-BUV805 (HI30, BD), hCD3-PECyn7 (SK7, BD), hCD4-PerCP (RPA-T4, Biolegend), hCD8-APC-H7 (SK1, BD), hKi67-AF700 (B56, BD), hCD270-BV421 (cw10, BD), and mCD45-BUV395 (30-F11, BD). For intracellular staining, Foxp3/Transcription Factor Staining Buffer Set (eBioscience) was used. Cells were washed with 1X PBS before acquisition on an X20 cytometer (Becton Dickinson (BD), San Jose, CA). For PC3 and clone 1B11 experiments, the absolute count of different populations was determined by adding 50 µL of Cell Counting Beads (Bangs Laboratories) just before acquisition. For MDA and Gerlach experiments, CD4+ and/or CD8+ T-cell counts were calculated from counts of tumor cells susensions determined with a Luna automatic counter (LogosBio), relative to $CD4^+$ and/or $CD8^+$ T-cell frequencies within total cells, as determined by flow cytometry. Data were analyzed using FlowJo software (TreeStar, Ashland, OR, USA).

*Statistical analysis*

All statistical tests were performed with Prism software (Graph Pad Inc, La Jolla, CA, USA). To compare ranks between two groups, the p-value was calculated with a non-parametric two tailed Mann-Whitney t-test. Survival analyses were performed with a log-rank (Mantel-Cox) test. Statistical modelling of tumor growth was performed by non-linear regression using the exponential growth model. The p-values of these tests are indicated on each panel. Statistical power of the analyses (alpha) was arbitrarily set at 0.05. No a priori test were performed to adequate the number of samples with statistical power.

## Results

### Treatment of humanized mice grafted with PC3 tumor with anti-HVEM is associated with a reduction of tumor growth and an increase in TIL number and proliferation

To evaluate the efficacy of an anti-HVEM therapy in a human context, NSG mice were engrafted with PC3, an HVEM-positive prostate cancer cell line (Figure 1A). Tumor growth was significantly reduced in mice treated with the 18.10 antibody compared to controls, an effect that could already be observed after a single injection (Figure 1B). Of note is that Graft-vs-Host Disease that occurs in immuno-compromised mice grafted with human cells was not affected by the treatment, as documented by a similar mortality in the two groups (Figure 1B). Flow cytometry analysis of human tumor-infiltrating lymphocytes (TIL) revealed an increase in CD4 T-cells numbers and a similar tendency for CD8 T-cells (Figure 1C). Additionally, frequencies of cells expressing the proliferation marker Ki67 were significantly elevated in both CD4 and CD8 T-cells (Figures 1D). Overall, anti-HVEM therapy in humanized mice decreased the growth of the PC3 cell line, associated to an increase in TIL numbers and proliferation.

### HVEM expression by the tumor is required for treatment efficacy

Before injection, we monitored HVEM expression by human PBMC and found that HVEM was highly expressed by human T and B cells (Figure 2A). Thus, the therapeutic effect described above could be due to an agonist effect of the mAb on HVEM-expressing T cells, leading to improved proliferation and numbers. Alternatively, the antibody could target HVEM on the tumor and block necessary survival signals and/or induce apoptosis. To discriminate between these two hypotheses, we generated an HVEM-deficient cell line derived from PC3 using CRISPR-Cas9 technology. Cleavage assay was performed to determine genome editing efficiency. Transfection of CRISPR-Cas9/sgRNA complex resulted in 30% of cleavage efficiency, corresponding to 4% of cells affected on two alleles (Figure S1A). After subcloning, we obtained several clones with undetectable surface expression of HVEM (Figure S1B), from which 1B11 was chosen for further experiments given its morphological similarity with wild-type PC3 (Figure S1C). However, the treatment with anti-HVEM mAb was ineffective at controlling the growth of 1B11 in humanized mice (Figure 2B), indicating an essential role for HVEM expressed by the tumor. In line with that result, similar numbers and frequencies of $Ki67^{+}$ cells in TIL from treated or control groups were observed in mice grafted with the 1B11 clone (Figures 2C-D), suggesting that the mAb had no agonist activity on human T cells in this experimental context.

**NSG myeloid cells are able to kill wild-type PC3 cells in presence of the anti-HVEM antibody**

Knowing that HVEM expression by the tumor was crucial for the efficacy of the mAb, we evaluated whether the mAb would be able to directly kill tumor cells. To that end, we engrafted PC3 wild-type and clone 1B11 in non-humanized NSG mice and monitored tumor growth following mAb administration. Interestingly, a reduction in tumor growth was observed for wild-type PC3, although the effect was less marked that in humanized mice (Figure 3A). In contrast, no difference in tumor growth was observed for the clone 1B11 with anti-HVEM therapy (Figure 3B). Thus, the mAb had a mild toxic effect on the cell line in the absence of human T cells, suggesting a direct effect mediated by HVEM. However, *in vitro* assays showed that the anti-HVEM mAb was unable to induce tumor cell death by itself (Figure 3C). Thus, the lower tumor growth *in vivo* was probably not due to a direct killing effect of the mAb.

Because NSG mice are on a NOD genetic background which is deficient for complement activity (20), we surmised that innate immunity of NSG mice might be involved in the activity of the mAb. To assess the participation of myeloid cells in the anti-tumor response, we injected the anti-Gr1 mAb during the anti-HVEM treatment to deplete neutrophils and macrophages of the NSG. An unexpected weight loss and mortality of the mice treated with anti-Gr1 was observed (Figure S2A-B). However, there was a trend for an abolition of the effect of the HVEM mAb in anti-Gr1-treated mice compared to controls (Figure S2C). More significantly, co-cultures of PC3 cells with peritoneal cells from NSG mice, which were mostly macrophages (Figure S3), resulted in an increased proportion of dead cells in the culture in presence of the anti-HVEM mAb (Figure 3D). Importantly, this effect was not observed with the HVEM-deficient cell line 1B11 (Figure 3E). The ability of macrophages from NSG mice to induce apoptosis of tumor cells was confirmed using live imaging of the co-cultures, with a significant increase in the number of apoptotic tumor cells overtime in presence of the anti-HVEM mAb compared to the isotype control (Figures 3F). Furthermore, examination of video microscopy of the co-cultures revealed that tumor cells were killed by contact with NSG peritoneal macrophages with no evidence for engulfment of tumor cells (Video S1). Altogether, these results show that NSG peritoneal macrophages were able to rapidly kill HVEM-expressing tumor cells in presence of the anti-HVEM mAb by a cell-contact dependent mechanism.

**The anti-tumor effect of the anti-HVEM mAb is not restricted to the PC3 cell line in humanized mice**

In light of the therapeutic effect of anti-HVEM on PC3 tumor growth, we sought to determine whether this observation could be extrapolated to other type of tumors. As expected, no difference in tumor growth or TIL numbers were observed with mice grafted with the breast cancer cell line MDA-MB-231, which does not express HVEM (Figure 4A-C). In contrast, a significant reduction of

tumor growth and a tendency for an elevated number of TIL in mice grafted with the HVEM$^+$ Gerlach melanoma cell line were observed (Figure 4D-F), as with the PC3 cell line.

## Discussion

Here, we report for the first time the efficacy of anti-HVEM therapy in humanized mice in various tumor models. We also bring some clues about the mechanisms involved in this anti-tumor effect.

Targeting HVEM with an antibody may possibly acts on tumor growth through four non-mutually exclusive mechanisms: (i) blockade of the interaction between tumor HVEM and its ligands expressed on immune cells (especially BTLA and CD160 for T-cells) should nullify inhibition of T-cell activation and consequently allow T cell proliferation and possibly improved functions, (ii) stimulation of HVEM on tumor by an agonist mAb may also promote tumor cell death directly, as it has been reported that in some circumstances HVEM may induce apoptosis despite the absence of intracellular death domains (22), (iii) tumor cell death may be caused by FcR-dependent mechanisms too, depending of the isotype used (23), (iv) stimulation of HVEM signaling on T-cells by an agonist mAb may promote proliferation and functions, and finally enhance killing of tumor cells.

Surprisingly, we identified myeloid cells of NSG mice as key players in the mode of action of the mAb, confirming published observations in syngeneic mouse models that myeloid cells are crucial for tumor control upon immune checkpoints inhibitors treatment (24–26). NSG mice are reported to have no T-cells, no B-cells, no NK-cells owing to the SCID and γc mutations, and no complement and defectives DC and macrophages owing to the NOD genetic background (27). Here, using 3 complementary techniques, we showed that killing of tumor cells by peritoneal macrophages from NSG mice was enhanced in presence of the anti-HVEM mAb, providing a possible mechanism to explain better control of tumor growth *in vivo* with or without human T cells. Because of the murine nature of the mAb, binding to murine Fc-receptors present on myeloid cells of NSG might have propelled the therapeutic efficacy of the mAb. In our setting, we used IgG1, that is reported to bind to CD16 (FcgRIII) and CD32 (FcgRIIB), activating and inhibitory receptors, respectively (28). However, NOD background has been associated with a strong decrease in FcgRIIB expression by macrophages (29). Consequently, activating FcgRIII might be the main receptor involved in FcR-dependent activity of murine myeloid cells in NSG mice. Several possibilities exist to explain tumor killing by myeloid cells, through antibody-dependent cellular phagocytosis (ADCP), local secretion of free radicals and many others (30,31). We did not see evidence for ADCP on the video microscopies collected during the course of this study. Thus, the exact mechanism by which myeloid cells killed the tumor in presence of the mAb remains to be elucidated.

An important observation that we made using CRISPR/Cas9 abolition of HVEM expression, was that the expression of HVEM by the tumor was strictly required for therapeutic efficacy. Thus, one can

infer that HVEM expression by human cells play little or no role in our model. Indeed, no effect of the mAb on human T cells was observed if the tumor was HVEM-negative and we didn't observe any difference in the occurrence of GVHD in our mice, suggesting that our antibody was unable to directly stimulate T-cells though HVEM. In contrast, Park *et al.* showed in a syngeneic mouse model that transfecting an agonist scFv anti-HVEM on tumors cells resulted in an increase in T-cell proliferation, as well as improved IFN-γ and IL-2 production and better tumor control (17). This discrepancy could be explained by the fact that T-cells are strongly activated in huPBMC mice (32). Since HVEM is downregulated upon activation (33), it may have limited binding of anti-HVEM antibody on T-cells in our model. Thus, it remains possible that the mAb is still endowed with agonist properties *in vitro* or that it would behave differently in another model or in humans. On the other side, BTLA is also upregulated upon T-cell activation (33), so the anti-HVEM mAb might also have limited inhibition of activated T-cells through inhibition of the HVEM-BTLA axis, allowing T cell proliferation on tumor site and consequently, associated with FcR-dependent tumor death, better control of tumor growth. Likewise, previous studies in mice showed a positive effect on T-cells of inhibiting HVEM expression by the tumor or its interaction with its ligands. Injection of a plasmid encoding a soluble form of BTLA (to compete for HVEM) was associated with an increase inflammatory cytokines production by TIL and a decrease of anti-inflammatory cytokines at the RNA level (18). Moreover, silencing of tumor HVEM with siRNA was also associated with an increase in CD8 T cells and inflammatory cytokine production in a murine colon carcinoma model (12). In addition, use of siRNA to HVEM on ovarian cancer *in vitro* promote T-cells proliferation and TNF-α and IFN-γ (19). Thus, our data suggest the following model to explain the antitumor activity of our anti-HVEM antibody in NSG mice: binding of the mAb on HVEM expressed by the tumor would (i) activate murine myeloid cells, and that would (ii) generate immune cell death that would (iii) enhance T-cell response.

Scheduled treatment with an anti-human HVEM mAb in humanized mice exerted a potent anti-tumor effect on the two HVEM$^+$ tumor cell lines tested, opening the possibility to apply this therapy to a wide range of solid cancers where HVEM is overexpressed (11–15,34–39). The recent success of ICI for cancer immunotherapy (anti-CTLA-4, anti-PD-1/PD-L1) has confirmed the hypothesis that the immune system can control many cancers. In light of the promising results reported herein, anti-HVEM therapy might be combined with ICI to further enhance anti-tumor immunity.

**Acknowledgment and disclosure**

This study was supported by Cancéropôle Île-de-France and Association pour la recherche sur les tumeurs de la prostate (ARTP).

S.B. was supported by a doctoral fellowship from the French Ministère de l'Education Supérieure et de la Recherche.

N.A. is supported by a doctoral fellowship from the Fondation ARC pour la recherche sur le cancer.

P.KC. is supported by a doctorate fellowship from the Institut Universitaire de Cancérologie (Sorbonne Université).

D.O.'s team was supported by the grant "Equipe FRM DEQ201802339209". D.O. is Senior Scholar of the Institut Universitaire de France.

Conflict of interest: D.O. is cofounder and a shareholder of Imcheck Therapeutics.

## References

1. Hanahan D, Weinberg RA. Hallmarks of cancer: the next generation. Cell. 2011 Mar 4;144(5):646–74.

2. Mittal D, Gubin MM, Schreiber RD, Smyth MJ. New insights into cancer immunoediting and its three component phases — elimination, equilibrium and escape. Curr Opin Immunol. 2014 Apr;27:16–25.

3. Hargadon KM, Johnson CE, Williams CJ. Immune checkpoint blockade therapy for cancer: An overview of FDA-approved immune checkpoint inhibitors. Int Immunopharmacol. 2018 Sep 1;62:29–39.

4. Havel JJ, Chowell D, Chan TA. The evolving landscape of biomarkers for checkpoint inhibitor immunotherapy. Nat Rev Cancer. 2019 Mar;19(3):133.

5. Park Y-J, Kuen D-S, Chung Y. Future prospects of immune checkpoint blockade in cancer: from response prediction to overcoming resistance. Exp Mol Med. 2018 Aug 22;50(8):109.

6. Cai G, Anumanthan A, Brown JA, Greenfield EA, Zhu B, Freeman GJ. CD160 inhibits activation of human CD4+ T cells through interaction with herpesvirus entry mediator. Nat Immunol. 2008 Feb;9(2):176–85.

7. Sedy JR, Gavrieli M, Potter KG, Hurchla MA, Lindsley RC, Hildner K, et al. B and T lymphocyte attenuator regulates T cell activation through interaction with herpesvirus entry mediator. Nat Immunol. 2005 Jan;6(1):90.

8. Pasero C, Speiser DE, Derré L, Olive D. The HVEM network: new directions in targeting novel costimulatory/co-inhibitory molecules for cancer therapy. Curr Opin Pharmacol. 2012 Aug 1;12(4):478–85.

9. Cheung TC, Steinberg MW, Oborne LM, Macauley MG, Fukuyama S, Sanjo H, et al. Unconventional ligand activation of herpesvirus entry mediator signals cell survival. Proc Natl Acad Sci U S A. 2009 Apr 14;106(15):6244–9.

10. Harrop JA, McDonnell PC, Brigham-Burke M, Lyn SD, Minton J, Tan KB, et al. Herpesvirus entry mediator ligand (HVEM-L), a novel ligand for HVEM/TR2, stimulates proliferation of T cells and inhibits HT29 cell growth. J Biol Chem. 1998 Oct 16;273(42):27548–56.

11. Inoue T, Sho M, Yasuda S, Nishiwada S, Nakamura S, Ueda T, et al. HVEM Expression Contributes to Tumor Progression and Prognosis in Human Colorectal Cancer. Anticancer Res. 2015 Jan 3;35(3):1361–7.

12. Migita K, Sho M, Shimada K, Yasuda S, Yamato I, Takayama T, et al. Significant involvement of herpesvirus entry mediator in human esophageal squamous cell carcinoma. Cancer. 2014;120(6):808–17.

13. Lan X, Li S, Gao H, Nanding A, Quan L, Yang C, et al. Increased BTLA and HVEM in gastric cancer are associated with progression and poor prognosis. OncoTargets Ther. 2017 Feb 16;10:919–26.

14. Hokuto D, Sho M, Yamato I, Yasuda S, Obara S, Nomi T, et al. Clinical impact of herpesvirus entry mediator expression in human hepatocellular carcinoma. Eur J Cancer. 2015 Jan 1;51(2):157–65.

15. Tsang JYS, Chan K-W, Ni Y-B, Hlaing T, Hu J, Chan S-K, et al. Expression and Clinical Significance of Herpes Virus Entry Mediator (HVEM) in Breast Cancer. Ann Surg Oncol. 2017 Dec 1;24(13):4042–50.

16. M'Hidi H, Thibult M-L, Chetaille B, Rey F, Bouadallah R, Nicollas R, et al. High Expression of the Inhibitory Receptor BTLA in T-Follicular Helper Cells and in B-Cell Small Lymphocytic Lymphoma/Chronic Lymphocytic Leukemia. Am J Clin Pathol. 2009 Oct 1;132(4):589–96.

17. Park J-J, Anand S, Zhao Y, Matsumura Y, Sakoda Y, Kuramasu A, et al. Expression of anti-HVEM single-chain antibody on tumor cells induces tumor-specific immunity with long-term memory. Cancer Immunol Immunother. 2012 Feb 1;61(2):203–14.

18. Han L, Wang W, Fang Y, Feng Z, Liao S, Li W, et al. Soluble B and T Lymphocyte Attenuator Possesses Antitumor Effects and Facilitates Heat Shock Protein 70 Vaccine-Triggered Antitumor Immunity against a Murine TC-1 Cervical Cancer Model In Vivo. J Immunol. 2009 Dec 15;183(12):7842–50.

19. Zhang T, Ye L, Han L, He Q, Zhu J. Knockdown of HVEM, a Lymphocyte Regulator Gene, in Ovarian Cancer Cells Increases Sensitivity to Activated T Cells. Oncol Res Featur Preclin Clin Cancer Ther. 2016 Jul 18;24(3):189–96.

20. Shultz LD, Schweitzer PA, Christianson SW, Gott B, Schweitzer IB, Tennent B, et al. Multiple defects in innate and adaptive immunologic function in NOD/LtSz-scid mice. J Immunol. 1995 Jan 1;154(1):180–91.

21. Gertner-Dardenne J, Fauriat C, Orlanducci F, Thibult M-L, Pastor S, Fitzgibbon J, et al. The co-receptor BTLA negatively regulates human Vg9Vd2 T-cell proliferation: a potential way of immune escape for lymphoma cells. 2013;122(6):11.

22. Costello RT, Mallet F, Barbarat B, Schiano de Colella J-M, Sainty D, Sweet RW, et al. Stimulation of non-Hodgkin's lymphoma via HVEM: an alternate and safe way to increase Fas-induced apoptosis and improve tumor immunogenicity. Leukemia. 2003 Dec;17(12):2500–7.

23. Bakema JE, van Egmond M. Fc receptor-dependent mechanisms of monoclonal antibody therapy of cancer. Curr Top Microbiol Immunol. 2014;382:373–92.

24. Dhupkar P, Gordon N, Stewart J, Kleinerman ES. Anti-PD-1 therapy redirects macrophages from an M2 to an M1 phenotype inducing regression of OS lung metastases. Cancer Med. 2018;7(6):2654–64.

25. Gordon SR, Maute RL, Dulken BW, Hutter G, George BM, McCracken MN, et al. PD-1 expression by tumor-associated macrophages inhibits phagocytosis and tumor immunity. Nature. 2017 May 25;545(7655):495–9.

26. Gubin MM, Esaulova E, Ward JP, Malkova ON, Runci D, Wong P, et al. High-Dimensional Analysis Delineates Myeloid and Lymphoid Compartment Remodeling during Successful Immune-Checkpoint Cancer Therapy. Cell. 2018 Nov 1;175(4):1014-1030.e19.

27. Shultz LD, Lyons BL, Burzenski LM, Gott B, Chen X, Chaleff S, et al. Human Lymphoid and Myeloid Cell Development in NOD/LtSz-scid IL2Rγnull Mice Engrafted with Mobilized Human Hemopoietic Stem Cells. J Immunol. 2005 May 15;174(10):6477–89.

28. Bruhns P. Properties of mouse and human IgG receptors and their contribution to disease models. Blood. 2012 Jun 14;119(24):5640–9.

29. Luan JJ, Monteiro RC, Sautès C, Fluteau G, Eloy L, Fridman WH, et al. Defective Fc gamma RII gene expression in macrophages of NOD mice: genetic linkage with up-regulation of IgG1 and IgG2b in serum. J Immunol. 1996 Nov 15;157(10):4707–16.

30. Furness AJS, Vargas FA, Peggs KS, Quezada SA. Impact of tumour microenvironment and Fc receptors on the activity of immunomodulatory antibodies. Trends Immunol. 2014 Jul 1;35(7):290–8.

31. Gül N, Egmond M van. Antibody-Dependent Phagocytosis of Tumor Cells by Macrophages: A Potent Effector Mechanism of Monoclonal Antibody Therapy of Cancer. Cancer Res. 2015 Dec 1;75(23):5008–13.

32. Ali N, Flutter B, Rodriguez RS, Sharif-Paghaleh E, Barber LD, Lombardi G, et al. Xenogeneic Graft-versus-Host-Disease in NOD-scid IL- 2Rcnull Mice Display a T-Effector Memory Phenotype. PLOS ONE. 2012;7(8):10.

33. Murphy KM, Nelson CA, Šedý JR. Balancing co-stimulation and inhibition with BTLA and HVEM. Nat Rev Immunol. 2006 Sep;6(9):671.

34. Ren S, Tian Q, Amar N, Yu H, Rivard CJ, Caldwell C, et al. The immune checkpoint, HVEM may contribute to immune escape in non-small cell lung cancer lacking PD-L1 expression. Lung Cancer. 2018 Nov 1;125:115–20.

35. Tang M, Cao X, Li Y, Li G-Q, He Q-H, Li S-J, et al. High expression of herpes virus entry mediator is associated with poor prognosis in clear cell renal cell carcinoma. Am J Cancer Res. 2019 May 1;9(5):975–87.

36. Sideras K, Biermann K, Yap K, Mancham S, Boor PPC, Hansen BE, et al. Tumor cell expression of immune inhibitory molecules and tumor-infiltrating lymphocyte count predict cancer-specific survival in pancreatic and ampullary cancer. Int J Cancer. 2017;141(3):572–82.

37. Sideras K, Biermann K, Verheij J, Takkenberg BR, Mancham S, Hansen BE, et al. PD-L1, Galectin-9 and CD8+ tumor-infiltrating lymphocytes are associated with survival in hepatocellular carcinoma. OncoImmunology. 2017 Feb 1;6(2):e1273309.

38. Zhu Y-D, Lu M-Y. Increased expression of TNFRSF14 indicates good prognosis and inhibits bladder cancer proliferation by promoting apoptosis. Mol Med Rep. 2018 Sep;18(3):3403–10.

39. Mochizuki K, Kawana S, Yamada S, Muramatsu M, Sano H, Kobayashi S, et al. Various checkpoint molecules, and tumor-infiltrating lymphocytes in common pediatric solid tumors: Possibilities for novel immunotherapy. Pediatr Hematol Oncol. 2019 Feb;36(1):17–27.

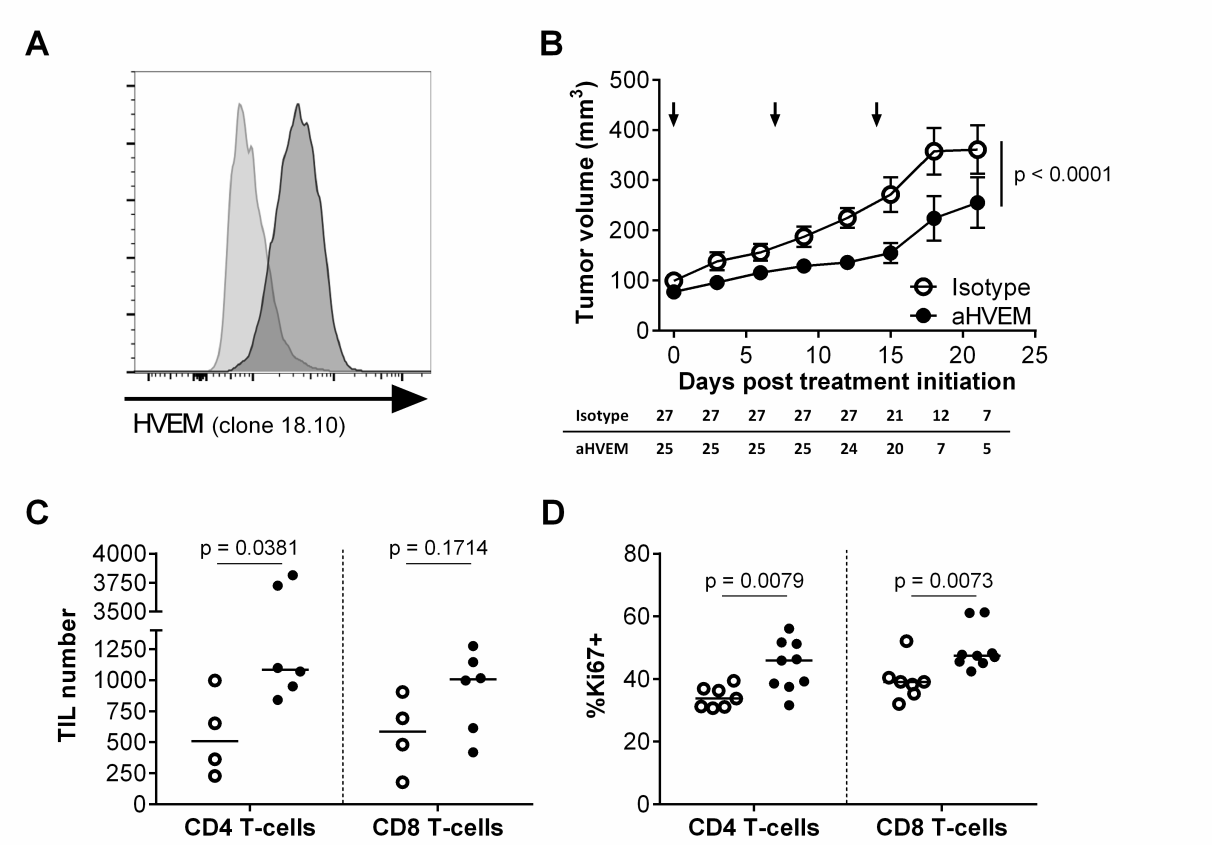


**Figure 1: Treatment of humanized mice grafted with PC3 tumor with anti-HVEM is associated with a reduction of tumor growth and an increase in TIL number and proliferation** (A) HVEM expression on PC3 cells revealed with anti-HVEM (clone 18.10) and secondary antibody. (B) Tumor growth of PC3 cell line grafted in humanized mice treated with anti-HVEM (as described in material and methods). Curves are the mean tumor volume (±SEM). Number of mice in each group at each time is indicated in the table below the graph. Data are cumulative of 4 independent experiments. Arrows indicate the time of injection. (C) Total number of $CD4^+$ and $CD8^+$ T-cells in tumors from one representative experiment. Numbers were determined by flow cytometry using Cell Counting Beads. (D) Frequencies of Ki67-expressing cells among $CD4^+$ and $CD8^+$ T-cells cumulative of two independent experiments.

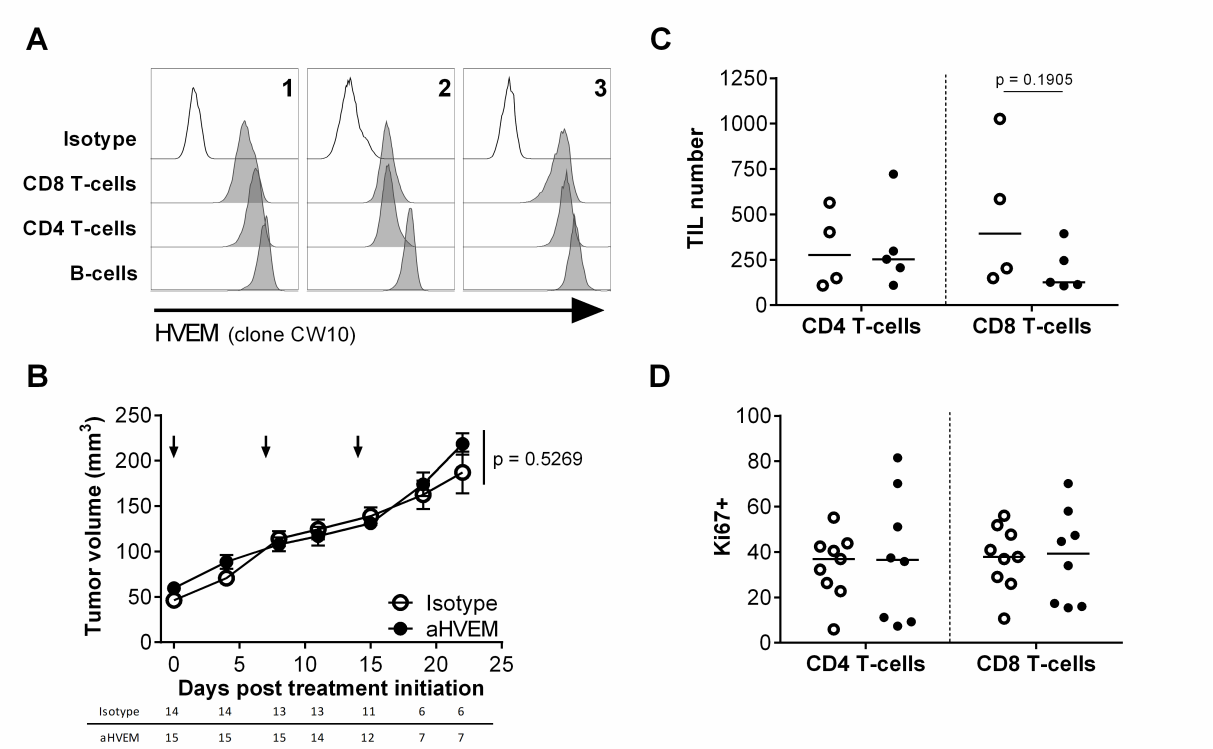


**Figure 2: HVEM expression by the tumor is required for treatment efficacy** (A) Expression of HVEM on PBMC before injection to mice (from 3 different human donors). (B) Tumor growth of clone 1B11 grafted in humanized mice treated with anti-HVEM. Data are cumulative of 2 experiments and represents the mean tumor volume (±SEM). Number of mice at each time is indicated in the table below the graph. Arrows indicate the time of injections (C) Total number of $CD4^+$ and $CD8^+$ T-cells in tumors from one representative experiment. (D) Percentage of Ki67-expressing cells among $CD4^+$ and $CD8^+$ T-cells from two different experiments.

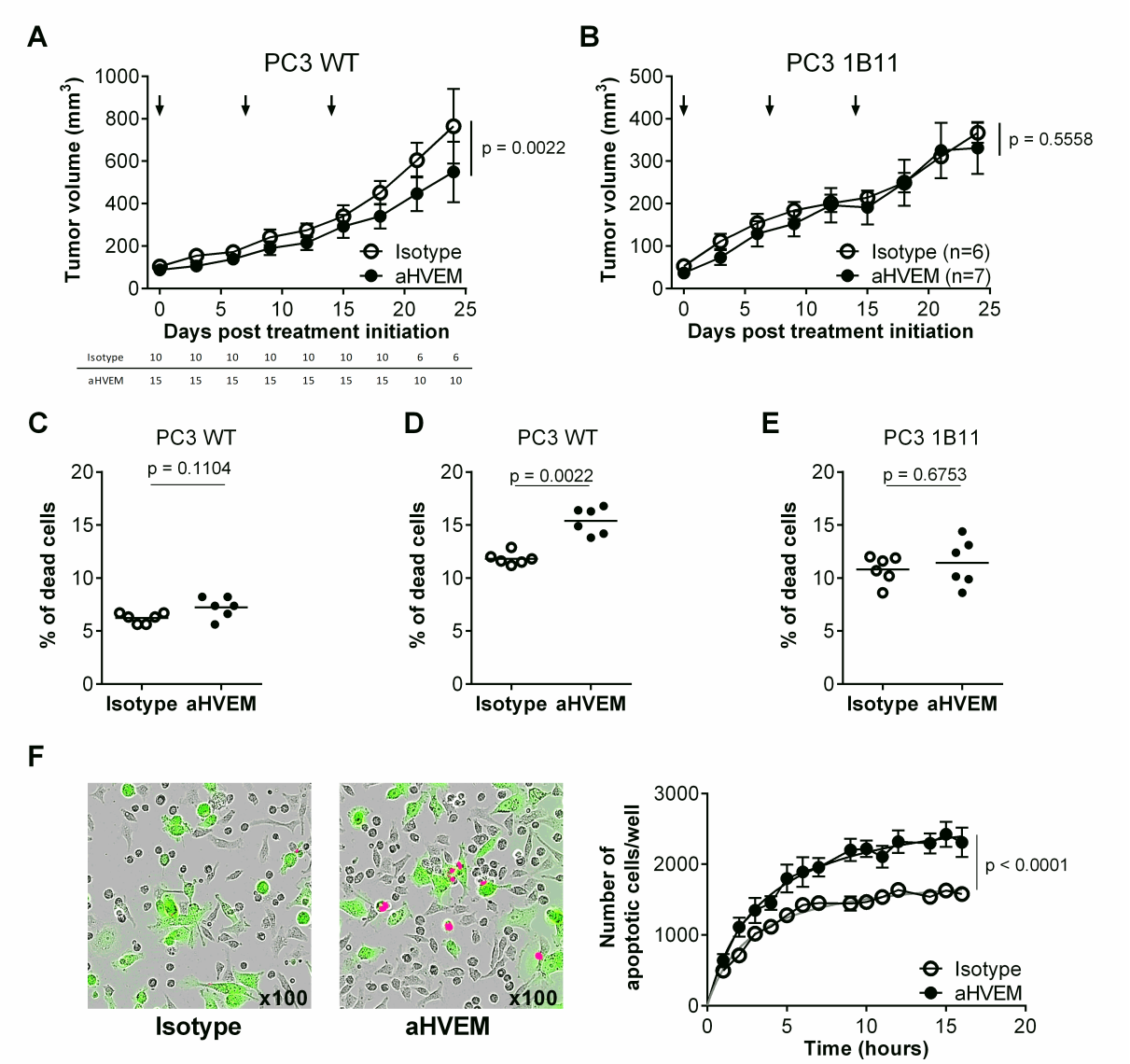


**Figure 3: NSG myeloid cells are able to kill wild-type PC3 cells in presence of the anti-HVEM antibody** (A, B) Tumor growth of wild-type (PC3 WT) and HVEM-negative PC3 clone (PC3 1B11) cell lines in non-humanized NSG mice. Numbers are cumulative of respectively 3 and 2 experiments and represents the mean tumor volume (±SEM). Number of mice at each time is indicated in the table below the graph. Arrows indicate the time of injection. (C) Frequencies of dead cells of wild-type PC3 cells (PC3 WT) in culture with anti-HVEM or isotype control or (D) with NSG peritoneal macrophages or (E) with HVEM-negative PC3 cells and macrophages. (F) GFP-expressing wild-type PC3 cells were co-cultured with NSG peritoneal macrophages and an apoptosis staining reagent. Culture was monitored during 16 hours by Incucyte and overlapping of GFP (green) and apoptosis staining (red) was quantified and reported as number of apoptotic cells/well. Depicted are the results from one representative experiment out of two.

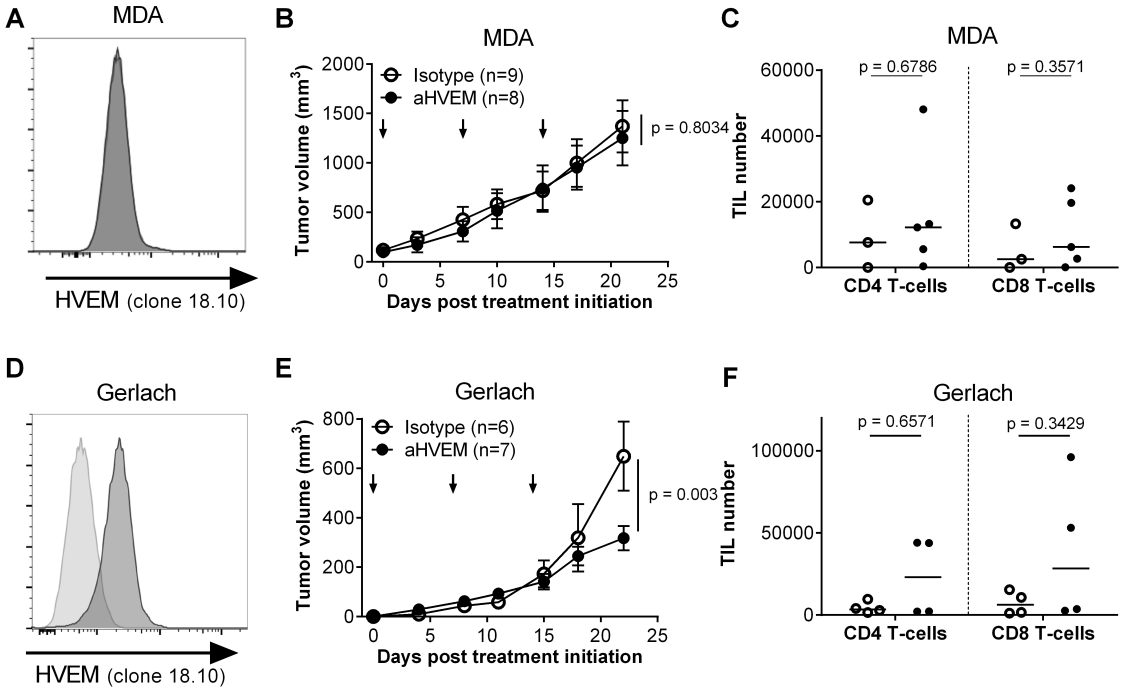


**Figure 4: The anti-tumor effect of the anti-HVEM mAb is not restricted to the PC3 cell line in humanized mice** (A, D) HVEM expression on MDA-MB-231 (MDA) and Gerlach cells revealed with anti-HVEM (clone 18.10) and secondary antibody. (B, E) Tumor growth of MDA-MB-231 and Gerlach cell lines grafted in humanized mice treated with anti-HVEM (as described in material and methods). Curves represents the mean tumor volume (±SEM) from one experiment. Numbers of mice at the beginning of the experiment are indicated in brackets. (C, F) Total TIL numbers in MDA-MB-23 and Gerlach in humanized mice.